Density Depletion at Solid–Liquid Interfaces: a Neutron Reflectivity Study

ARTICLE *in* LANGMUIR · FEBRUARY 2007

Impact Factor: 4.46 · DOI: 10.1021/la061943y · Source: PubMed

Density Depletion at Solid−Liquid Interfaces: a Neutron Reflectivity Study

M. Maccarini,*,†,‡,▽ R. Steitz,§ M. Himmelhaus,† J. Fick,† S. Tatur,|| M. Wolff,£,⊥ M. Grunze,*,† J. Janeček,# and R. R. Netz#

Institut für Angewandte Physikalische Chemie, Ruprecht Karls Universität Heidelberg, Im Neuenheimer Feld 253, D-69120, Heidelberg, Germany, FZK, Institut für Nukleare Entsorgung, Postfach 3640, D-76021 Karlsruhe, Germany, Hahn-Meitner-Institut, Glienicker Strasse 100, D-14109 Berlin, Germany, Institut Laue-Langevin, 6, rue Jules Horowitz, BP 156 - 38042 Grenoble Cedex 9, France, Université de Montreal, Centre de Recherche, CHUM - Hôtel-Dieu, Montreal, Canada, Lehrstuhl für Festkörperphysik/ EP IV, Ruhr-Universität Bochum, Bochum, Germany, and Physik Department, Technische Universität München, James Franck Strasse, D-85748 Garching, Germany

Received July 5, 2006. In Final Form: September 24, 2006

Neutron reflectivity experiments conducted on self-assembled monolayers (SAMs) against polar (water) and nonpolar (organic) liquid phases reveal further evidence for a density reduction at hydrophobic−hydrophilic interfaces. The density depletion is found at the interface between hydrophobic dodecanethiol (C12) and hexadecanethiol (C16) SAMs and water and also between hydrophilic SAMs (C12/C11OH) and nonpolar fluids. The results show that the density deficit of a fluid in the boundary layer is not unique to aqueous solid−liquid interfaces but is more general and correlated with the affinity of the liquid to the solid surface. In water the variation of pH has only minor influence, while different electrolytes taken from the Hofmeister series seem to increase the depletion. On hydrophobic SAMs an increase in density depletion with temperature was observed, in agreement with Monte Carlo simulations performed on corresponding model systems. The increase in the water density depletion layer is governed by two effects: the surface energy difference between water and the substrate and the chemical potential of the aqueous phase.

Introduction

A close relationship exists between the density of a liquid in the vicinity of a surface and the solvation force appearing between two surfaces immersed in the liquid.[1] This is of particular importance for hydrophobic objects in water, since the resulting force—the *hydrophobic interaction*—is responsible for key biological phenomena such as protein folding, self-assembly, colloids stability, and membrane fusion.[2,3] Lum, Chandler, and Weeks[4] presented a unified theory of solvation which is applicable to small and extended nonpolar objects in water. The theory was developed in terms of a general treatment of excluded volume effects. Small nonpolar particles can be dissolved in water because they can be fitted into the hydrogen-bonded network since the entropic cost paid by the water molecules associated with the loss of conformational freedom is lower than the energetic cost of breaking a hydrogen bond. When the size of the hydrated nonpolar object is larger than a few nanometers, the situation changes; hydrogen-bonding between water molecules in the direct vicinity of hydrophobic surface becomes energetically unfavorable. This induces a density reduction of the interfacial liquid so that two extended hydrophobic surfaces in close proximity will attract each other due to pressure imbalance between the bulk and confined water.

Further insight in hydrophobic interactions comes from computer simulations in which the bond strength and orientation of water molecules at the surface can be correlated to the water density in the interface and the resulting hydration forces. A layer of water with reduced density, which from now on will be called *depletion* layer, was found in molecular dynamics (MD) simulations performed on a planar hydrophobic substrate consisting of a dense layer of alkane molecules oriented normal to the interface.[5] The depletion layer can be quantified in terms of the depletion distance,[5] D, which is the normalized integral difference between the actual density across the interface and the corresponding bulk densities on both sides of the interface. The values of the depletion layer D derived from experiments and theoretical calculations can be quantitatively compared.[5] The MD simulations in ref 5 were performed at different radii of curvature of the hydrophobic alkane layer and at different temperatures. The resulting depletion distance was significantly affected by the temperature and ranged from 2.13 Å at $T = 273$ K to 2.95 Å at $T = 360$ K. In contrast, the effect of pressure was less pronounced. Pertsin and Grunze[6] performed grand canonical Monte Carlo simulations (GCMC) on asymmetric slitlike nanopores, formed by two walls, one hydrophilic and one hydrophobic. In the vicinity of the hydrophobic wall, a depletion layer was found whose extension depends significantly on the chemical potential of water. As it approaches the value

* To whom correspondence should be addressed. E-mail: marco.maccarini@mcgill.ca. (M.M.); michael.grunze@urz.uni-heidelberg.de (M.G.).

† Ruprecht Karls Universität Heidelberg.

‡ Institut für Nukleare Entsorgung.

§ Hahn-Meitner-Institut.

£ Institut Laue-Langevin.

|| Université de Montreal.

⊥ Ruhr-Universität Bochum.

Technische Universität München.

▽ Current address: Department of Chemistry, McGill University McGill University, 801 Sherbrooke St. West, Room PP 109, Montreal Quebec H3A2K6, Canada.

(1) Attard P.; Berard D. R.;. Ursenbach C. P.; and Patey G. N. *Phys. Rev. A* **1991**, *44*(12), 8224.

(2) Israelachvili, J.; Wennerström, H. *Nature (London)* **1996**, *379*, 219.

(3) Yaminsky, V. V.; Vogler E. A. *Curr. Opin. Colloid Interface Sci.* **2001**, *6*, 342−349.

(4) Lum, K.; Chandler, D.; Weeks, J. D. *J. Phys. Chem. B* **1999**, *103*, 4750.

(5) Mamatkulov, S. I.; Khabibullaev, P. K.; Netz, R. R. *Langmuir* **2004**, *20*, 4750.

(6) Pertsin, A.; Grunze, M. *J. Phys. Chem. B* **2004**, *108*, 16533−16539.

10.1021/la061943y CCC: $37.00
Published on Web 11/22/2006

corresponding to liquid−gas coexistence, the density of water in the confinement fluctuates, strongly indicating a metastable situation.

In computer simulations the results depend on the approximations and the potential functions used to describe the interactions between the water molecules themselves and the walls. For example, the hydration forces can vary significantly when orientation-dependent contribution are included in the water−wall potential or the rigidity of the surface groups involved in H-bond interaction[7] is varied. Therefore, measuring the density of water at the interface is crucial to verify or falsify the calculated correlations between the properties of the solid (surface energy, surface composition), the properties of the liquid phase (pH, electrolyte concentration), and the interfacial water density and hydration forces.

One technique that is particularly useful in measuring liquid density at a solid interface is neutron reflectometry (NR). Changing the contrast by isotopic substitution[8] can enhance the sensitivity to the small difference in water density in the water/solid interphase. The latter is particularly important since it was shown that more invasive methods such as surface force measurements and AFM can induce artifacts such as "nanobubbles".[9,10]

Although a water depletion layer at hydrophobic surfaces was confirmed experimentally by various neutron and X-ray reflectometry experiments, the reported results on its thickness and its dependence on the properties of the surfaces and the liquid phase vary considerably. NR experiments performed on deuterated polystyrene films[9] in contact with D_2O gave evidence of a depletion layer with $D \approx 2.6$ Å. The effect of dissolved gas was studied on an octadecyl-trichlorosilane (OTS) monolayer adsorbed on quartz resulting in a depletion distance $D \approx 2.6$ Å for degassed D_2O that increases to $D \approx 3.1$ Å when the liquid was exposed for 18 h to air.[11] A consistently higher value of $D \approx 24$ Å was found in a NR experiment performed on octadecanethiol self-assembling monolayers (SAMs) adsorbed on gold in contact with D_2O,[12] although precautions were taken to avoid contaminations and degassed water was used. In the other extreme, X-ray experiments of water in contact with a paraffin film[13] gave a depletion layer of $D \approx 1$ Å. The strong variation of the measured thickness of depletion layer at hydrophobic surfaces may be due to the different nanoscale roughness of these surfaces which cannot be unambiguously accounted for in the fitting routines for the reflectivity profiles.

In the work presented here, NR experiments were used to probe the water density in the solid/liquid interface by varying the interfacial energy between the solid and the liquid phase. Also, the effects of pH, temperature, and electrolytes were probed. We chose to work with SAMs of alkanethiolates on gold surfaces. This choice is motivated by the fact that alkanethiol SAMs allows a precise control over the surface properties.[14,15] This SAM system was pre-characterized in detail and showed high stability in water[16] and in contact with organic solvents.

The use of SAMs on a gold layer of tens of nanometers was also dictated by sensitivity concerns. Preliminary NR experiments performed on hydrophobic silicon substrates proved to be not sensitive enough to detect the presence of the depletion layer. In systems comprised of one thin interfacial layer, its contribution to the reflectivity profiles can be detected only at high momentum transfer, Q, where the errors are large due to the fact that the reflected intensity is approaching the background signal of diffuse scattering. Therefore, at high Q, the detection of small variations in interphase density can be prohibitively long to achieve a reasonable signal-to-noise ratio. Hence, in our experiments a gold film of typically 500 Å thickness was evaporated on a quartz crystal coated with a thin titanium adhesion promoter. The interference of the neutrons scattered by the interfaces of the subsequent layers causes a series of maxima and minima of the reflectivity as a function of the momentum transfer, the so-called Kiessig fringes. The distance of two adjacent maxima and the intensity of the peaks is very sensitive to the properties of the subsequent layers that contribute to the reflectivity profile at all Q.

The paper is organized as follows. We first summarize the details of our experiments and the procedures used to fit the reflectivity curves in order to obtain information on the density of the solid/liquid interfaces studied. A brief description of the Monte Carlo simulation used to complement the experiments is also given. Then we show the results obtained for hydrophobic and hydrophilic surfaces in contact with water and nonpolar solvents, the effect of varying pH and electrolytic composition, and the dependence on the temperature, followed by a discussion of the results and the conclusions.

Experimental Details

Chemicals. Deuterated dodecanethiols (C12) and hexadecanethiols (C16) were synthesized according to the procedure described by Urquhart et al.[17] The perdeuterated alkylhalogenide were ordered from C/D/N Isotopes, Canada, with a degree of deuteration of 98%. Dodecanethiol (C12), 11-mercapto-1-undecanol (C11OH) was purchased from Sigma-Aldrich, deuterium oxide 99.9%, *d*-cyclohexane 99.9%, *d*-toluene 99.9% from Deutero GmbH, and ethanol absolute, hydrogen peroxide, sulfuric acid, *N*,*N*-dimethylformamide, and hydrochloric acid were received from Sigma-Aldrich, with "per analysis" purity.

Materials. Polished single-crystal SiO_2(0001) substrates ($8.9 \times 3.8 \times 1.3$ cm^3) were purchased from CrysTec Berlin, Germany, and coated with a thermally evaporated 200−500 Å thick Au (99.99%) film. A 20−50 Å Ti interlayer was used to promote Au adhesion. The typical root-mean-square (rms) roughness of the metallic substrate was between 8 and 12 Å, as measured by AFM.

Monolayer Preparation and Characterization. All glassware used to prepare the samples were left overnight in hydrogen peroxide and rinsed in ethanol p.a. The freshly evaporated gold substrates were sonicated in dimethylformamide for 5 min prior to UV cleaning with a UV lamp for 2 h. Immediately after the UV irradiation, the substrates were immersed in ethanol for at least 10 min in order to avoid oxidation which might result in the formation of isolated multilayer islands, as reported by Woodward et al.[18] The gold substrates were then immersed in a 1 mM solution of dodecanethiol in ethanol overnight and sonicated for 5 min in order to remove the physisorbed thiols. The thickness of the films was measured with an M-44 spectral ellipsometer from J. A. Woollam Co., Inc., the advancing contact angles were measured with a Krüss G1 goniometer

(7) Hayashi, T.; Pertsin, A. J.; Grunze, M. *J. Chem. Phys.* **2002**, *117*, 6271.
(8) Lu, J. R.; Thomas, R. K. *J. Chem. Soc., Faraday Trans.* **1998**, *94*(8), 995.
(9) Steitz, R.; Gutberlet, T.; Hauss, T.; Klosgen, B.; Krastev, R.; Schemmel, S.; Simonsen, A. C.; Findenegg, G. H. *Langmuir* **2003**, *19*, 2409−2418.
(10) Gleb, E.; Yakubov, H.-J. B.; Vinogradova, O. I. *J. Phys. Chem. B* **2000**, *104*, 3407−3410.
(11) Doshi, D. A.; Watkins, E. B.; Israelachvili, J. N.; Majewski, J. *PNAS* **2005**, *102*, 27, 9458.
(12) Schwendel D.; Hayashi T.; Dahint R.; Pertsin, A.; Grunze, M.; Steitz, R.; Schreiber F. *Langmuir* **2003**, *19*(6), 2284−2293.
(13) Jensen, T. R.; Jensen, M. O.; Reitzel, N.; Balashev, K.; Peters, G. H.; Kajer, K.; Bjornholm T. *Phys. Rev.Lett.* **2003**, *90*(8), 086101.
(14) Ulman, A. *Thin Solid Films* **1996**, *273*, 48−53.
(15) Silin, V. I.; Wieder, H.; Woodward J. T.; Valincius, G.; Offenhausser, A.; Plant, A. L *J. Am. Chem. Soc.* **2002**, *124*, 14676.
(16) Maccarini, M.; Himmelhaus, M.; Stoycheva, S.; Grunze, M. *Appl. Surf. Sci.* **2005**, *252*, 1941−46.
(17) Urquhart, G. C.; Gates, J. W.; Connor, R. *Organic Syntheses*, Collective Vol. 3; Wiley: New York, 1955; p 363.
(18) Woodward, J. T.; Walker, M. L.; Meuse, C. W.; Vanderah, D. J.; Poirier, G. E.; Plant, A. L. *Langmuir* **2000**, *16*, 5347−535.

using purified deionized water (Milli-Q plus system, Millipore, Eschborn, Germany). AFM measurements were performed with a Park Autoprobe (Veeco Instruments) operated in contact mode and equipped with a 5 μm × 5 μm scanner. Roughness values were calculated as rms deviations from the mean height using built-in software. The films were further characterized by grazing-angle fourier transform infrared spectroscopy (FTIR) performed by a Bruker Optics IFS66v spectrometer.

Experimental Procedure. The NR measurements were performed at the Berlin Neutron Scattering Center at the Hahn-Meitner Institut on the V6 reflectometer[19] and at the Institut Laue-Langevin on the Adam reflectometer. To record one reflectivity curve took 9−12 h at the V6 and 5−7 h at the Adam reflectometer, during which the surface had to be stable and free of contaminations. The V6 instrument operates on cold neutrons at a wavelength of $\lambda = 4.66$ Å and a resolution ranging from 0.001 to 0.002 Å^{-1} dependent on collimation. The Adam reflectometer[20] works with a neutron wavelength of 4.41 Å and was used with a fixed resolution of 0.0005 Å^{-1}. The data collected were footprint-corrected to account for the change of the sample surface area exposed to the neutron beam as the incident angle was varied and normalized to the measured incident intensity. The background was determined by measuring for each sample the off-specular reflectivity and subtracted (in the experiments at the V6 instrument) or accounted for in the analysis (in the experiments at the Adam reflectometer).

NR measurements were first done in the dry state by placing the samples in an aluminum cell connected with a vacuum pump that allowed for a pressure of about 10^{-5} mbar in order to obtain the thicknesses, the scattering length density (SLD), and the roughness of the Au and Ti layers. The samples were then measured in contact with the liquids by using homemade sample cells made of Teflon and sealed with Viton O-rings. The design was adapted from similar cells used by Howse and co-workers.[21] Prior to the measurements, water and deuterium oxide were degassed for about 20 min in a glass flask connected to a vacuum pump. A Teflon stirrer was used to promote the nucleation of air bubbles that were successively removed by the applied vacuum. Temperature-dependent measurements were performed with a homemade aluminum cell sealed with Viton O-rings due to the higher thermal conductivity of this metal compared with Teflon.

Particular care was devoted to the preparation of the sample and to the cleaning procedures for the experimental cells since adsorption of contaminants on the surface can alter the reflectivity profile of the interfacial region. The Teflon cell was left several hours in piranha solution (1/3 hydrogen peroxide, 2/3 concentrated sulfuric acid) and then rinsed for several hours in an ultrasonic bath with Millipore water. The aluminum cell was cleaned in an ultrasonic bath with ethanol, an ethanol/chloroform mixture, and chloroform. All plastic connectors and syringes were left in a solution of Millipore water and Decon overnight and then rinsed in an ultrasonic bath for several hours in Millipore water before use.

The samples were characterized by ellipsometry, IR spectroscopy, contact angle measurements, and XPS. A critical aspect of these experiments was the stability of the surfaces in water, which has been studied in previous work.[16]

Substrate Parameters. The parameters used to describe the substrate were the thickness of the layers i, d_i, the SLD of the layers ρ_i, and the roughness between subsequent layers $\sigma_{i,i+1}$. The values of ρ_{Au} and ρ_{Quartz} were taken from the literature.[12,22] The value of ρ_{Ti} was fitted to the experiments taken in a vacuum to account for the unavoidable hydrogen contamination during the thermal evaporation deposition of that layer. It is known that due to the high solubility and diffusivity of hydrogen in Ti, hydrogen contamination shifts the SLD of this material to lower values.[23] Also the SLD of the bulk liquids, $\rho_{bulk,liq}$, was fitted to account for the errors in the mixtures of deuterated and protonated components and the possible presence of H_2O in the D_2O. The $\rho_{bulk,liq}$ were obtained by fitting the reflectivity profiles in a restricted interval around Q_c, the momentum transfer corresponding to the total internal reflection, since this value depends only on the SLD of the first (quartz) and the last (liquid) layer. For measurements with liquids index matched to gold, the total internal reflection occurs at too small Q to be measured. In these cases, the $\rho_{bulk,liq}$ were determined by measuring the reflectivity profiles of the liquid against a silicon substrate. The $\rho_{bulk,liq}$ obtained deviated at most by 1.5% from their stoichiometric values.

Data Analysis. The reflectivity curves were analyzed by standard neutron optical methods[24] based on Parratt's formalism for reflectivity of stratified media.[25] The interface system is divided in a suitable number of layers of constant SLD, and the reflectivity is calculated by applying dynamical scattering theory. The optimal thickness, roughness, and scattering length densities of the subsequent layers are then obtained by least-squares fitting procedures. Two problems were encountered in the fitting procedures of the systems under study: the first was related to the resolution of the layers (I), the second to the roughness of the layers (II).

(I) A distinct layer can easily be resolved if its thickness is larger than the $2\pi/Q_{max}$, where Q_{max} is the maximum momentum transfer achieved in the reflectivity experiment conducted. With $Q_{max} \leq 0.2$ Å^{-1} in our case, the minimum thickness directly observable is $d_{min} \geq 30$ Å. This implies that at least for C12 and C11OH the first minimum of the respective interference (Kiessig fringe) of the SAMs is beyond the accessible Q_{max}.

(II) Commonly, interlayer roughness is accounted for by replacing the steplike function of the SLD of two successive layers with an error function profile as suggested by Nevot and Croce.[26] Their method is valid as long as the thickness of the layer is significantly larger than the roughness of the interface. In the case of our ultrathin organic monolayers on Au films, this condition is not fulfilled since thickness and roughness of the SAMs are both of the order of 10 Å.

The fitting strategy used to fit the data for the short C12 SAM on Au had to take into account both potential problems. This was done by combining the SAM with $\rho_{SAM} < \rho_{bulk,liq}$ and the possible adjacent depletion layer with $\rho_{interph,liq} < \rho_{bulk,liq}$ in a single box of thickness d_L, with SLD ρ_L and zero roughness. In other words, we merged the entire interfacial layers (i.e., the rough gold surface, the organic monolayer and the interfacial liquid) into a single layer as described in Figure 1. Assuming that the interfacial roughness throughout the surface layers is not strongly affected by the liquid (water or a nonpolar solvent), the difference in the reflectivity profiles can then be ascribed to differences in the fluid density at the SAM/liquid interface.

To compare the interfacial density profile in the different experiments we calculated the depletion distance[5] defined as

$$D = \int \mathrm{d}z \left(1 - \frac{\rho_{hc}(z)}{\rho_{hc,bulk}} - \frac{\rho_{liq}(z)}{\rho_{liq,bulk}}\right) \quad (1)$$

where $\rho_{hc}(z)$ and $\rho_{liq}(z)$ are the densities of the hydrocarbons and of the liquid respectively, and $\rho_{hc,bulk}$ and $\rho_{liq,bulk}$ their respective bulk densities. In the case of a single-box model with zero roughness, eq 1 can be approximated by

$$D \approx d_L \frac{\rho_{liq,bulk} - \rho_L}{\rho_{liq,bulk}} \quad (2)$$

(19) Mezei, F.; Goloub, R.; Klose, F.; Toews, H. *Physica B* **1995**, *213/214*, 898.
(20) Schreyer, A.; Siebrecht, R.; Englisch, U.; Pietsch, U.; Zabel, H. *Physica B* **1998**, *248*, 349.
(21) Howse, J. R.; Manzanares-Papayanopolous, E.; McLure, I. A.; Bowers, J.; Steitz, R.; Findenegg, G. H. *J. Chem. Phys.* **2002**, *116*, 7177.
(22) Russell, T. P. *Mater. Sci. Rep.* **1990**, *5*, 171.
(23) Krist, T.; Brière, M.; Cser, L. H in Ti thin films. *Thin Solid Films* **1993**, *228*, (Issues 1−2), 141−144.
(24) Braun, C. Parratt32 Fitting routine for reflectivity data. Ph.D. Thesis, HMI, Berlin, 1997−1999.
(25) Parratt, L. G. *Phys. Rev.* **1954**, *95*, 359.
(26) Nevot, L.; Croce, P. *Rev. Phys Appl.* **1980**, *15*, 761.

Table 1. Fitting Parameters for Sample S1 (Mixture of Hydrogenous and Deuterated Dodecanethiols) against H_2O/D_2O, C_6H_{12}/C_6D_{12} Mixtures, S2 (Deuterated Dodecanethiol) against D_2O and *d*-Octane, and S3 (Mixture of Hydrogenous 11-Mercapto-1-undecanol and Deuterated Dodecanethiol) in Contact with H_2O/D_2O and Toluene/*d*-Toluene Mixture

sample	S1+H_2O/D_2O	S1+C_6H_{12}/C_6D_{12}	S2 + D_2O	S2 + *d*-octane	S3+H_2O/D_2O	S3 + tol/*d*-tol
d_L[Å]	33 ± 3	32 ± 4.5	21.02 ± 5	15.25 ± 5	38.85 ± 4	43.23 ± 3
ρ_L [$\times 10^{-6}$Å^{-2}]	3.31 ± 0.1	3.73 ± 0.1	5.42 ± 0.2	5.70 ± 0.2	3.40 ± 0.1	3.44 ± 0.1
$\rho_{liq,bulk}$ [$\times 10^{-6}$Å^{-2}]	4.04 ±0.1	4.36 ± 0.1	6.37 ± 0.1	6.38 ± 0.1	4.21 ± 0.1	4.4 ± 0.1
χ^2	1×10^{-2}	1.85×10^{-2}	$5.2 \times 10-2$	7.2×10^{-2}	3.35×10^{-2}	1.97×10^{-2}
D [Å]	6.0 ±1.2	4.6 ± 1.1	3.1 ± 1	1.6 ± 0.75	7.5 ± 1.4	9.4 ± 1.4
ΔD [Å]	1.4 ± 1.6		1.5 ± 1.3		−1.9 ± 1.9	

Table 2. Fitting Parameters for Sample S1 (Mixture of Hydrogenous and Deuterated Dodecanethiols) against C_6H_{12}/C_6D_{12}, H_2O/D_2O (pH 5), H_2O/D_2O (pH 2), and in the Presence of $CaCl_2$ and K_2SO_4

sample	S1+C_6H_{12}/C_6D_{12}	S1+H_2O/D_2O (pH 5.5)	S1+H_2O/D_2O (pH 2)	S1+H_2O/D_2O ($CaCl_2$)	S1+H_2O/D_2O (K_2SO_4)
d_L [Å]	32 ± 4.5	33 ± 3	37.2 ± 3	41.28 ± 4	38.8
ρ_L [$\times 10^{-6}$Å^{-2}]	3.73 ± 0.1	3.31 ±0.1	3.29 ± 0.1	3.19 ± 0.1	3.24
$\rho_{liq,bulk}$ [$\times 10^{-6}$Å^{-2}]	4.36 ± 0.1	4.04 ±0.1	3.9 ±0.1	3.74 ± 0.1	3.9
χ^2	1.85×10^{-2}	1×10^{-2}	1.07×10^{-2}	1.48×10^{-2}	1.34×10^{-2}
D [Å]	4.6 ± 1.1	6.0 ± 1.2	5.9 ± 1.4	6.1 ± 1.5	6.5 ± 1.4
ΔD [Å]	−	1.4 ± 1.6	1.2 ± 1.7	1.5 ± 1.9	1.9 ± 1.8

Table 3. Fitting Parameters for Sample S4 (Deuterated Hexadecanethiols) against D_2O at Temperatures of 6, 25, and 50 °C for the Two Fitting Strategies Used, Fit Method I and Fit Method II

sample	S4 $T = 6$ °C fit method I	S4 $T = 6$ °C fit method II	S4 $T = 25$ °C fit method I	S4 $T = 25$ °C fit method II	S4 $T = 50$ °C fit method I	S4 $T = 50$ °C fit method II
ρ_{SAM} [$\times 10^{-6}$Å^{-2}]	5.66	5.48	5.5	5.39	5.52	5.41
d_{SAM} [Å]	16	27	16	27	16	27
d_L [Å]	16 ± 4	15.09 ± 4	23.25 ± 6	19.73 ± 5	23.6 ± 6	18.6 ± 5
ρ_L [$\times 10^{-6}$Å^{-2}]	5.48 ± 0.2	5.73 ±0.2	5.68 ± 0.2	5.77 ± 0.15	5.53 ± 0.16	5.63 ± 0.1
$\rho_{liq,bulk}$ [$\times 10^{-6}$Å^{-2}]	6.29 ± 0.1	6.29 ± 0.1	6.27 ± 0.1	6.27 ± 0.1	6.25 ± 0.1	6.25 ± 0.1
χ^2	2.71×10^{-2}	2.37×10^{-2}	3.14×10^{-2}	2.67×10^{-2}	3.15×10^{-2}	2.75×10^{-2}
D [Å]	2.1 ± 0.7	1.4 ± 0.6	2.2 ± 1	1.6 ± 0.7	2.7 ± 0.9	1.9 ± 0.6

The depletion distance, D, reduces the smeared-out density profile of the liquid to a steplike function that represents an equivalent layer of zero density. D was obtained by introducing d_L and ρ_L obtained from the fits in eq 2. The errors on these quantities (shown in Tables 1−3) were evaluated from the fits and correspond to a 10% increase in the χ^2. The error of D was then calculated by error propagation rules. Finally, the D obtained for the SAMs against water were compared to those against a reference system (nonpolar solvent) by defining $\Delta D = D$(water) − D(nonpolar solvent).

Alternatively, when longer fully deuterated C16 monolayers were used (see Effect of Temperature), their contribution to the reflectivity curve could be included explicitly by adding a corresponding layer between the interfacial liquid and the gold of thickness d_{SAM} and SLD ρ_{SAM}, and no comparison with a reference system was needed.

The reliability of our box-model was checked by using an alternative method—slicing the real space SLD profile of the interfacial region—as described in the literature.[9,27] Initially, the interfacial scattering density profile was fitted by also including the roughness into the Parratt algorithm. The continuous interfacial profile was then sliced in a set of individual layers 8 Å thick with zero roughness. The resulting SLD profile of the interfacial region was then fitted with the following function:

$$\rho(z) = \rho_1 - \sum_{i=1}^{2} \frac{\rho_i - \rho_{i+1}}{2}\left(1 + \mathrm{erf}\left(\frac{z - z_i}{2^{1/2}\sigma_i}\right)\right) \qquad (3)$$

where ρ_1 and ρ_3 correspond to the SLDs of the gold and of the bulk liquid, respectively, and z_i being the position of the i interface. The extracted parameters were used to achieve a meaningful SLD profile of the interface that in terms of the depletion length did not show any differences with the result obtained by the box-model used in our analysis.

The analysis of scattering experiments involves, in general, the so-called "phase problem", i.e., the solution of a given scattering problem is not unique and many models can match one experimental reflectivity curve. The number of solutions is reduced by applying boundary conditions, i.e., by introducing the given sequence and physical properties of the layers. To further reduce any remaining ambiguity, we performed experiments on the same stratified system with bulk liquid phases of different SLDs, $\rho_{bulk,liq}$, by mixing the respective hydrogenous and deuterated compounds. The analysis of the different reflectivity curves was then constrained to the same physical characteristics of the interface. By matching the SLD of the bulk liquid phase to the known SLD of the Au layer, we further enhanced the sensitivity of the NR experiments against the density-reduced interphase liquid layer.[9]

Computer Simulation. Monte Carlo simulations were performed in systems that resemble those studied in the NR experiments in order to confirm and reinforce the results obtained. The NP_zAT ensemble used had a constant number of particles, constant lateral dimension of the simulation box, and constant pressure in the z direction and temperature, and it is particularly suited to simulate liquid−liquid and solid−liquid interfaces since it allows proper relaxation of the densities of the coexisting phases and returns surface tensions very close to the experimental values.[28] The interaction site model used to describe the interactions between particles is pairwise additive and includes Lennard−Jones and Coulomb contributions:

$$u_{ij}(r) = 4\epsilon_{ij}\left[\left(\frac{\sigma_{ij}}{r}\right)^{12} - \left(\frac{\sigma_{ij}}{r}\right)^{6}\right] + \frac{1}{4\pi\epsilon_0}\frac{q_i q_j}{r} \qquad (4)$$

where σ and ϵ are characteristic parameters for the Lennard−Jones interaction, q stands for the partial charge of particular site, and r is the separation between sites i and j.

(27) Tolan, M. *X-ray scattering from soft-matter thin films: materials science and basic research*; Springer: Berlin, 1999.

(28) Zhang, Y.; Feller, S. E.; Brooks, B. R.; Pastor, R. W. *J. Chem. Phys.* **1995**, *103* (23), 10252.

The SPC/E force field[29] was used to model water, whereas toluene, cyclohexane, and the SAMs were modeled through the TraPPE parameters.[30,31] The bond lengths and angles were kept fixed, and the molecule of cyclohexane was considered only in the more stable chair conformation. The interaction parameters are listed in Table A4 of the Supporting Information. The parameters for unlike pairs of sites were obtained using the Lorentz−Berthelot combining rules: $\sigma_{ij} = (\sigma_{ii} + \sigma_{jj})/2$ and $\epsilon_{ij} = (\epsilon_{ii}\epsilon_{jj})^{1/2}$. The Lennard−Jones interactions were truncated at a distance of 14 Å, and the long-range corrections were included according to a method recently suggested for inhomogeneous simulations.[32] In simulations of systems containing charged sites, the electrostatic interactions were treated using the Ewald technique for slab geometries.[33]

The SAMs were modeled as straight chains of united sites representing the methylene (and methyl or hydroxymethyl at the surface layers) groups; the united atom approach within the TraPPE model neglects the hydrogen atoms bonded to carbons, and the whole groups are considered as one single pseudoatom. The separation between the pseudoatoms was equal to 1.2916 Å, which corresponds to the projection of the length of the C−C bond (1.54 Å) on the axis of an alkane molecule in the all-trans conformation; thus the end-to-end distance of our model is equal to that of the real straightened chain. The chains are stacked up in hexagonal arrangement with a lattice constant $a = 5$ Å and tilt of 30° with respect to the normal direction so that the density of the model corresponds to the experimental density of a alkanethiolate SAM on a Au(111) surface. The positions of all these sites in the SAMs were kept fixed during the runs. Due to the used cutoff distance for nonbonded interactions, we could neglect also the presence of the gold and quartz layers. Within the used simplifications, the results of the simulations do not depend on the length of the hydrocarbon chain. To model the SAMs containing the hydroxyl groups, we replaced regularly two-thirds of the terminal CH_3 groups by OH groups. The ratio of CH_3 and OH groups 1:2 is close to experimentally observed 3:7. The hydroxyl groups were allowed to rotate freely around the C−O bond.

The lateral dimensions of the simulation box were 30.0×34.6410 Å^2. The liquid phase contained 2000 molecules of water or 343 molecules of toluene or cyclohexane. The thickness of the liquid films was about 50 Å. The SAM contained 48 chains in a regular hexagonal arrangement. Each chain was made of 15 segments representing the methylene, methyl, or hydroxyl groups. Periodic boundary conditions were applied in all the three directions. After 5×10^4 MC cycles to equilibrate the systems, one production run of 10×10^4 MC cycles was performed. The density profiles and the diagonal components of the virial tensor were evaluated and stored after every 10 MC cycles. The translational and rotational displacements were adjusted to get the acceptance ratio between 0.2 and 0.4. The change of the volume of the box was performed in the z direction only and also after every 10 MC cycles with desired acceptance about 25%. The temperature was 25 °C (298.15 K), and the external pressure applied in the z direction was 100 kPa. For water in contact with nonpolar SAMs, the simulations were performed also at 6 and 50 °C.

Results

C12 in Contact with H_2O/D_2O Mixtures and Nonpolar Solvents. The C12 SAMs prepared on the Au films had an advancing water contact angle of 107°. Experiments were carried out with two different films, one obtained from coadsorption of an equimolar mixture of hydrogenous and deuterated dodecanethiol SAM (S1) in contact with a liquid phase approximately index-matched to the gold layer, and the other one with a fully deuterated dodecanethiol SAM (S2) in contact with a fully deuterated liquid phase. The ellipsometric thickness of the two monolayers was 12 ± 0.6 Å. Figure 2a shows the reflectivity profiles of S1 in contact with a mixture of H_2O and D_2O (volume fraction of H_2O = 0.34), and in contact with a mixture of cyclohexane and deuterated cyclohexane (volume fraction of cyclohexane = 0.31) having approximately the same SLD. Fitting was performed by including the SAM and the interfacial liquid in a single box as discussed above. The extracted depletion distance, D, and the difference $\Delta D = D$(water) − D(organic solvent) between the depletion distance for water and the organic solvent are listed in Table 1 (The complete set of fitting parameters is listed in Table A1 of the supporting materials). In Figure 2b, the scattering length densities normalized to those of the respective bulk liquid phase are plotted. By comparing the depletion lengths measured in contact with those of water and cyclohexane, we find a relative density deficit for water in contact with the hydrophobic surface of $\Delta D = D$(water) − D(cyclohexane) = 1.4 Å. This relative density difference does not allow thecalculation of the true density deficit, D, in the interface for either water or the organic solvent since it considers both the SAM and the interface and can thus not be compared directly to previously

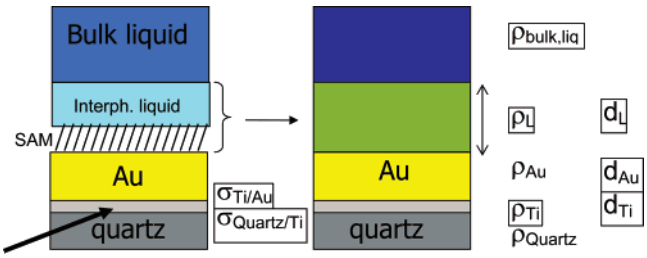

Figure 1. Schematic view of the multilayer system under investigation. Model parameters are listed on the right. Variable parameters are encircled with a frame. The thick arrow shows the direction of the incident neutron beam.

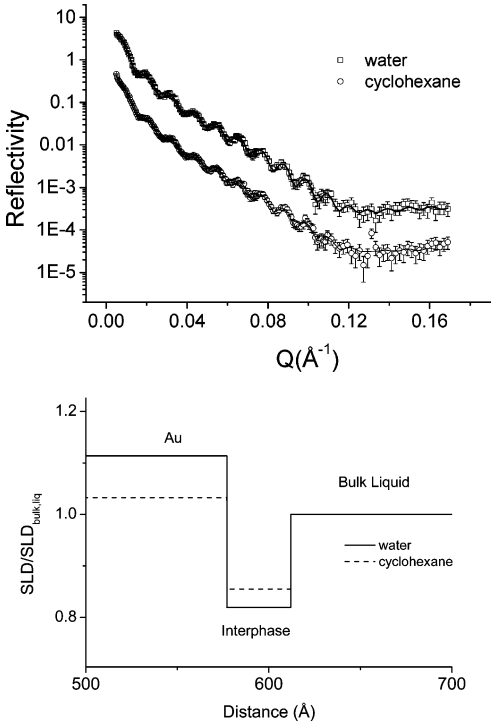

Figure 2. (a) Experimental reflectivity data and best fits (solid lines) for sample S1 against H_2O/D_2O, C_6H_{12}/C_6D_{12} mixtures. The data for water are offset on the y axis by a factor of 10 for clarity of presentation. (b) SLD of the interfacial region normalized to that of the bulk liquid for sample S1 against H_2O/D_2O, C_6H_{12}/C_6D_{12} mixtures.

(29) Berendsen, H. J. C.; Grigera, J. R.; Straatsma, T. P. *J. Phys. Chem.* **1987**, *91*, 6269.
(30) Martin, M. G.; Siepmann, J. I. *J. Phys. Chem. B* **1998**, *102*, 2569−2577.
(31) Wick, C. D.; Martin, M. G.; Siepmann, J. I. *J. Phys. Chem. B* **2000**, *104*, 8008−8016.
(32) Janecek, J. *J. Phys. Chem. B* **2006** (110), 6264−69.
(33) Yeh, I. C.; Berkowitz, M. L. *J. Chem. Phys.* **1999**, *111*, 3155.

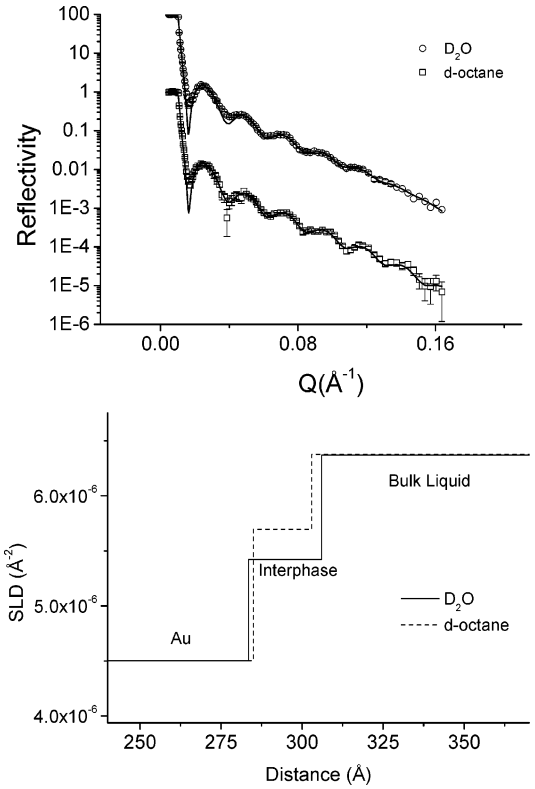

Figure 3. (a) Experimental reflectivity data and best fits (solid lines) for sample S2 against D_2O and *d*-octane. The data for D_2O are offset on the *y* axis by a factor of 100 for clarity of presentation. (b) SLD of the interfacial region of sample S2 against D_2O and *d*-octane.

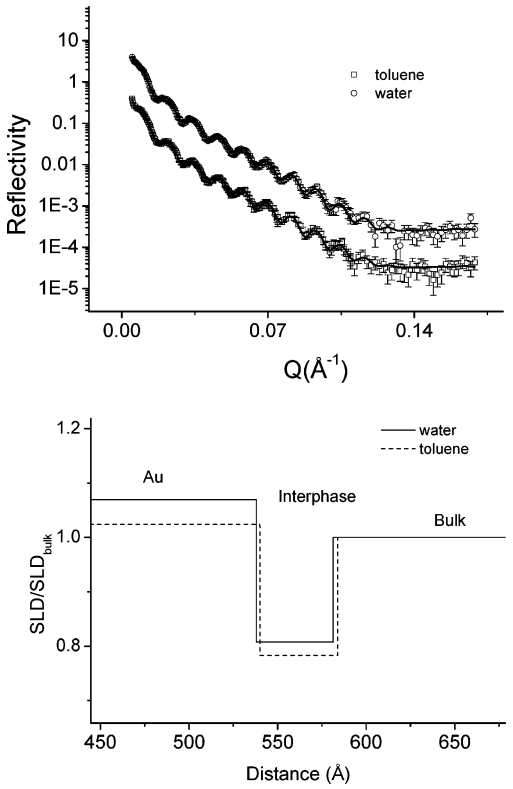

Figure 4. (a) Experimental reflectivity data and best fits (solid lines) for sample S3 against H_2O/D_2O, toluene/*d*-toluene mixtures. The data for water are offset on the *y* axis by a factor of 10 for clarity of presentation. (b) SLD of the interfacial region normalized to that of the bulk liquid for sample S3 against H_2O/D_2O, toluene/*d*-toluene mixtures.

reported data on the depletion layer. It is rather a relative measure for the different compatibility of the polar and nonpolar solvents with the substrate. Only if the SAMs were not affected by the different solvents and D would be zero for the organic liquid on the hydrophobic substrate, the density deficit for water would be directly comparable to previous experiments.[9,11,13]

To confirm the result, the experiment was repeated with a fully deuterated C12 SAM (S2) in contact with D_2O and *d*-octane. The reflectivity curves are shown in Figure 3a, and the extracted SLD profiles at the solid−liquid interfaces are plotted in Figure 3b. The result obtained ($\Delta D = 1.5$ Å) is in full agreement with those of the S1 film above.

We stress that using a reference system to extract the value of the density depletion was necessary because it was not possible to explicitly include in the fits the contribution of the short SAMs. By including the SAMs and the interfacial liquid in a single box, we introduced a dependence of D also on the SLD of the monolayer, which changes if different amounts of deuterated and hydrogenated alkanethiols are used. For sample S1 (50% mixture of deuterated and protonated SAMs) in contact with the aqueous phase, D was 6 Å, and for sample S2 (fully deuterated SAMs), D was 3.1 Å, while the respective ΔDs match within experimental error.

C11OH/C12 in Contact with H_2O/D_2O Mixtures and Nonpolar Solvent. NR was performed also on a more hydrophilic SAM (S3) obtained by immersing the gold substrate in a mixture of a 1 mM solution of C11OH and fully deuterated C12 at a ratio of 80:20 by volume. The relative concentration of the two molecules on the surface was measured by IR spectroscopy and gave a surface fraction of C12 of $\phi_{C12} = 0.3$. The advancing water contact angle was 45°, and the ellipsometric thickness was 12 ± 0.6 Å. The measurements against the liquid phase were conducted with a mixture of H_2O/D_2O and toluene/*d*-toluene. The reflectivity curves and the fits (performed with the same methodology as for the previous samples) are shown in Figure 4a, and the SLD normalized to SLD_{bulk} as a function of the distance from the interface is displayed in Figure 4b. We observe, contrary to the more hydrophobic surface, a density deficit of $\Delta D = D(\text{water}) - D(\text{toluene}) = -1.9$ Å of toluene as compared to water (see Table 1).

Effect of pH and Electrolyte. As reported by Schweiss et al.,[34] methyl-terminated alkanethiol SAMs undergo inversion of surface charge in contact with aqueous electrolyte solutions when the pH is lowered below 4.4. In particular, at pH > 4.4 the surface charge is negative, at pH 4.4 the surface charge is 0 (isoelectric point), and at pH < 4.4 the surface charge is positive. Sum frequency generation spectroscopy experiments showed that the surface charge of the SAM affects the orientation of the water molecules in contact with the organic monolayer[35,36] and thus might also induce density changes in the interfacial water. Contrary to expectation, the NR experiments on sample S1 at pH 5 and 2 (achieved by adding 5 μL of HCl (25%) to the H_2O/D_2O mixture) showed only small variation of the depletion distance with pH (Table 2).

The effect of salts taken from the Hofmeister series was also analyzed. This series reflects the capability of different salts to stabilize or precipitate protein solutions.[37] Although a molecular description of the mechanism involved is not yet conclusive,[38]

(34) Schweiss, R.; Welzel, P. B.; Werner, C.; Knoll, W. *Langmuir* **2001**, *17*, 4304−11.
(35) Kataoka, S.; Gurau, M. C.; Albertorio, F.; Holden, M. A.; Lim, S. M.; Yang, R. D.; Cremer, P. *Langmuir* **2004**, *20*, 1662.
(36) Du, Q.; Freysz, E.; Shen, Y. R. *Phys. Rew. Lett.* **1994**, *72*(2), 238.
(37) Hofmeister, F. *Arch. Exp. Pathol. Pharmakol.* **1888**, *24*, 247−260.

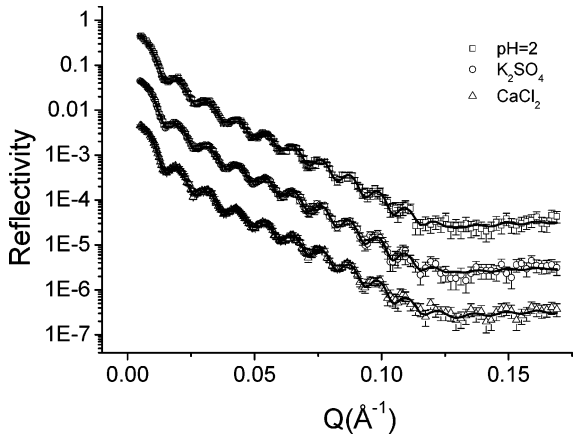

Figure 5. Experimental reflectivity data and best fits (solid lines) for sample S1 against H_2O/D_2O at pH 2 and in the presence of K_2SO_4 and $CaCl_2$. The data for the aqueous solutions of K_2SO_4 and $CaCl_2$ are offset on the *y* axis by a factor of 10^{-1} and 10^{-2}, respectively, for clarity of presentation.

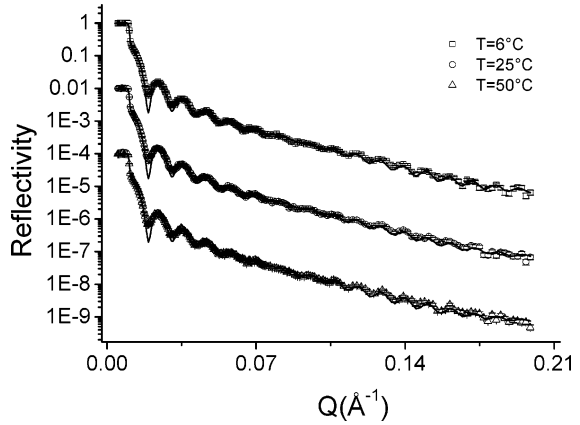

Figure 6. Experimental reflectivity data and best fits (solid lines) for sample S4 against D_2O at temperatures 6, 25, and 50 °C. The data for $T = 25$ and 50 °C are offset on the *y* axis by a factor of 10^{-2} and 10^{-4}, respectively, for clarity of presentation.

it is thought that the effect correlates with the ability of the salts to promote or disrupt the hydrogen-bonding network of water.[39] In our experiments, $CaCl_2$ was used as an example of a "*structure breaker*" and K_2SO_4 of a "*structure former*". The reflectivity profiles measured in contact with a 0.25 M $CaCl_2$ and K_2SO_4 aqueous solutions are shown in Figure 5, and the fitting parameters are listed in Table 2 (the complete list of fitting parameters is given in Table A2 of the Supporting Information). Both salts lead to an increased depletion distance as compared to pure water.

Effect of Temperature. The effect of temperature was investigated by measuring the reflectivity of a surface coated with fully deuterated hexadecanethiol (S4) in contact with D_2O at $T = 6$, 25, and 50 °C (Figure 6). The advancing contact angle of water on the surface measured at room temperature was 110°, and the ellipsometric thickness was 16 ± 0.8 Å. Compared to the previous experiments in which shorter dodecanethiols were used, the increased length of the fully deuterated molecule resulted in an observable reflectivity contrast between the SAM and the gold surface. Consequently, an extra box of thickness d_{SAM} and scattering length density ρ_{SAM} was added in the multilayer model between the interfacial region and the gold. Measurements against

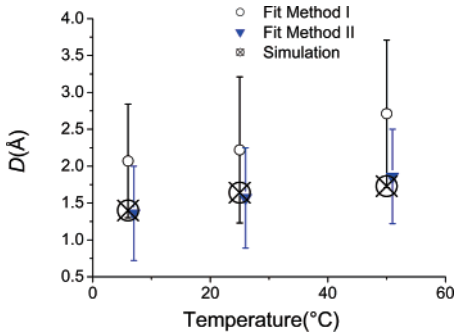

Figure 7. Depletion distance resulting from the analysis of the reflectivity data of sample S4 (deuterated hexadecanethiols) against D_2O as a function of temperature and with the two fitting strategies used. The results of the MC simulations are also shown for comparison.

Table 4. Depletion Distance and Wetting Coefficients Obtained from the Computer Simulations[a]

system	*D* [Å]	Δ*D* [Å]	wetting coeff
cyclohexane/nonpolar SAM	1.30		1.69
water/nonpolar SAM (25 °C)	1.64	0.34	(−0.3)−(−0.1)
toluene/polar SAM	1.04		1
water/polar SAM	0.25	−0.79	0.4−0.7
water/nonpolar SAM (6 °C)	1.40		
water/nonpolar SAM (25 °C)	1.64		(−0.3)−(−0.1)
water/nonpolar SAM (50 °C)	1.73		

[a] The errors on the depletion distance, *D*, are smaller than 0.05 Å.

a reference medium (nonpolar liquid) were not necessary to determine the density depletion of the interfacial liquid in this case. Note, that this procedure is identical to previous experiments in which the SAM and the water depletion layer were separately treated in the data evaluation.[11,12] However, although the thickness of the monolayer was higher than in the previously discussed samples (16 vs 12 Å), the roughness of the surface was still of the order of the thickness, so that the Nevot−Croce approach could not be applied.

Two fitting strategies were used in order to overcome this problem. In fit method I, the SLD of the SAMs, ρ_{SAM}, was also fitted and the thickness of the SAM, d_{SAM}, was instead kept fixed at its ellipsometric value. The SLD of the SAM monolayer resulting from the fit is between that of gold and that of deuterated methyl groups (~6.4×10^{-6} Å^{-2}). This is expected since the large surface roughness cannot be decoupled from the small thickness, and thus one measures an integrated value over the rough SAM/gold interface. The results listed in Table 3 indicate a depletion distance for water between 2.1 and 2.7 Å. The agreement with the results of the computer experiments is encouraging (see Figure 7).

In fit method II the thickness of the monolayer, d_{SAM}, was also fitted to account for the diffuse interface. To avoid unphysical solutions, the thickness of the Au−SAM layers was constrained to the value measured in vacuum. The χ^2 slightly improved and the SLD of the SAM determined from the fit was smaller as compared to the results obtained by fit method I (see Table 3 and Table A3 in the Supporting Information). The fits indicate the presence of a depletion layer of smaller extension as compared to that of fit method I. However, the trend with temperature is similar.

Computer Simulations. The results on the simulations are shown in Table 4. The thickness of the depletion layer was evaluated from the normalized density profiles (shown in Figures 8) according to eq 1.

The bulk number density of SAM phase depends on the used lattice parameters and is constant throughout the simulation; for

(38) Gurau, M. C.; Soon-Mi Lim, Castellana, E. T.; Albertorio, F.; Kataoka, S.; Cremer, P. S. *J. Am. Chem. Soc.* **2004**, *126*, 10522; Batchelor, J. D.; Olteanu, A.; Tripathy, A.; Pielak, G. J. *J. Am. Chem. Soc.* **2004**, *126*, 1958−1961.
(39) Cacace, M. G.; Landau, E. M.; Ramsden, J. J. *Quart. Rev. Biophys.* **1997**, *30*, 241−277.

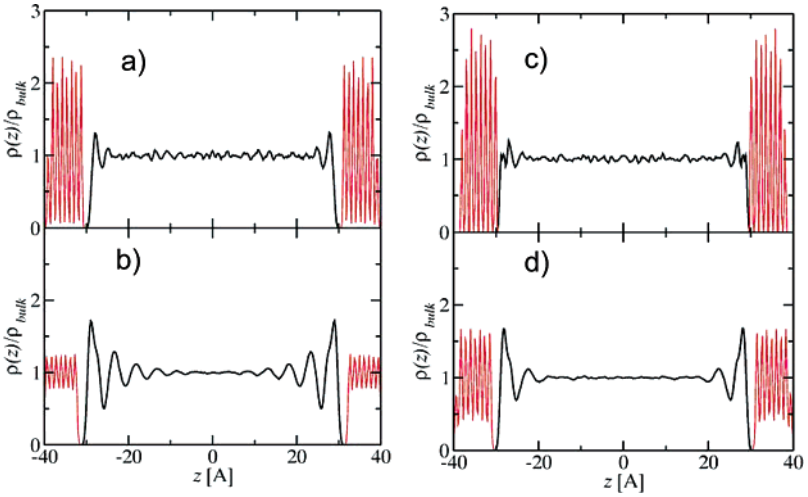

Figure 8. Normalized density profiles obtained in the Monte Carlo simulations (red lines SAMs, black lines liquids): (a) nonpolar SAM in contact with water, (b) nonpolar SAM in contact with cyclohexane, (c) polar SAM in contact with water, and (d) polar SAM in contact with toluene. Note that the simulations are performed at constant pressure and the z dimension of the boxes can vary. Fluctuations of the SAM box in this direction are related to the compressibility of the liquid in contact with them. The different compressibilities of water and the organic solvents are reflected in different SAM density profiles (peaks height and width) which, however, correspond to the same net density.

our model, it has a value 0.041 287 sites/Å^3. The densities of the fluids were obtained from inhomogeneous simulations of the corresponding vapor−liquid equilibrium.

The density obtained for toluene was 852 ± 1 kg/m^3 in good agreement with the experimental value of 862.3 kg/m^3. Similarly, for water the difference between the experimental value and the result of the simulation is smaller than 1% (simulation, 993 ± 1 kg/m^3 vs experimental, 997.004 kg/m^3). In the case of cyclohexane, the neglected flexibility of the six-carbon rings leads to a larger discordance (simulation, 760 ± 1 kg/m^3 vs experimental, 773.9 kg/m^3).[40] The wetting coefficients were calculated according to the well-known Young's equation

$$k = \cos\vartheta = -\frac{\gamma_{sg} - \gamma_{sl}}{\gamma_{lg}} \qquad (5)$$

where γ_{kj} is the interfacial tension between phase k and j (s, l, and g, stands for solid, liquid, and gaseous respectively). The difference in the numerator, $\gamma_{sg} - \gamma_{sl}$, is obtained from the simulations of the whole system. The values of surface tensions of pure liquids, γ_{lg}, are results of the inhomogeneous simulations of the vapor−liquid equilibrium of corresponding liquids. For toluene, we obtain 28.6 ± 0.4 mN/m (experimental value 27.93 mN/m), for water 66 ± 2 mN/m (experimental value 72.0 mN/m), and for cyclohexane 22.1 ± 0.9 mN/m (experimental value 24.35 mN/m). Even for very long simulation runs, the variations of the surface and interfacial tension values are quite large, especially in systems containing polar molecules (water). With respect to the error propagation, the uncertainties of the values of the wetting coefficients (and contact angles) are relatively broad.

In the case of nonpolar SAMs, a reduction of the depletion layer and a significant change of the wetting coefficient are observed if the water is replaced by cyclohexane (see Table 4). The value of the wetting coefficient for water at this SAM corresponds to a contact angle in the range 95−110°. For cyclohexane on this substrate, we obtained a value for the wetting coefficient smaller than −1 corresponding to complete wetting (spreading of the liquid on the interface); in a real experiment, a zero contact angle would be measured. This phenomenon can be explained by strong attraction between the particles of the two phases in contact. The mixing of both phases is prevented by fixing the positions of the SAM's molecules in the simulation.

For partially hydroxylated SAMs in contact with water or toluene, the obtained contact angles are in a rough agreement with experimental data, and a significantly lower thickness of the depletion layer for water as compared to the hydrophobic substrates is observed. This is caused by specific strong interaction between water molecules and hydroxyl groups (formation of hydrogen bonds). The sites in the molecule of toluene have no partial charge, and thus, they interact with the surface OH groups only through the Lennard−Jones interaction which is considerably weaker than the electrostatic interaction. Thus, the behavior of toluene on polar SAMs is not qualitatively different from its behavior on nonpolar SAMs.

The simulations of water in contact with nonpolar SAMs were also performed at three different temperatures, T = 6, 25, and 50 °C, as shown in Figure 7. The increase of the depletion distance with temperature is in fair agreement with the experiments.

Discussion

Problems and Errors. All experiments indicate a region of reduced density at the interface between water and the hydrophobic surfaces. First, we consider possible problems and errors which could obscure the experiments and the interpretation of the data. The adsorption of protonated contaminants on the surface, which, due to the low SLD would have the same effect on the reflectivity as a layer of fluid with reduced density, could be a source of error.[41] However, the adsorption of contaminants would have been detected in the ellipsometric measurements conducted on all samples before and after the NR experiment, and we also expect that the water contact angle would have been affected. From the surface characterization experiments conducted, we thus conclude that the samples were not contaminated or altered during the NR experiments. On three samples we detected contaminations, and the extension of the "depletion layer" in subsequent NR experiments was increasing with time and was not changing with temperature or electrolyte addition. These measurements were excluded from the presentation of data in this work.

(40) Janecek, J.; Krienke, H.; Schmeer, G. *J. Phys. Chem. B* **2006**, *110*, 6916−6923.

Another possible source of systematic error is the heterogeneity of the SAMs on the large substrates needed for the NR reflectivity experiments (surface area, 8.9 × 3.8 cm^2). The formation of the SAMs was performed according to techniques that should guarantee full surface coverage. The homogeneity of the SAMs was verified by performing contact angle measurements and ellipsometry on different parts of the surfaces. Within the errors of the measurements, the monolayer thickness and contact angle were the same.

The extraction of the structural parameters from the data involves several assumptions. Since the roughness of the gold substrate is of the same order as the thickness of the SAM, the Nevot−Croce approach to account for roughness in the fits could not be used. Hence, we performed experiments with water and with nonpolar solvents on the *same* SAM and assumed in our data evaluation that the molecular roughness of the SAM is not changed in the different solvents to an extent it would invalidate our approach. Sum Frequency Generation (SFG) spectroscopy experiments on various SAMs and polymer surfaces clearly show a solvent-induced reorientation of the molecules in the organic films and in some cases solvent penetration into the film,[42,43] but to which extent this influences the neutron reflectivity of the thin SAMs is not known. If the solvent induced only molecular reorientation, the effect on the density of the monolayer would hardly be visible with NR. The solvent molecules might also squeeze into the defects of the alkane chains of the films, with a net increase of the density of the film, but this would have a comparable effect in the hydrophilic and hydrophobic monolayers since the defect would expose the inner part of the alkane chain, so that a comparison of the results in the two cases is still meaningful. However, in view of this uncertainty, the *absolute* value of the depletion distances should be viewed with care.

Depletion Layer and the Affinity of Surface to Medium. The comparison of the results obtained in water and nonpolar solvents (cyclohexane and octane) indicate a density deficit in the case of an aqueous phase in contact with hydrophobic surfaces, which we ascribe to a layer of water with reduced density, as predicted by theoretical work by Lum et al.[4] and by the computer experiments of refs 5 and 6. The extension of the depletion layer in terms of ΔD is estimated to be ∼1.5 Å, close to the value found in the X-ray experiment by Jensen et al.[13] but smaller than that found in NR experiments performed on other systems.[9,11,12] Note again that this comparison is valid only if there are no solvent effects on the SAM and zero depletion in the SAM/organic liquid interface.

Interestingly, when NR was measured for a more hydrophilic surface in contact with water and a nonpolar solvent (toluene), a density deficit was observed in the latter case, which corresponds to a negative value of ΔD. This indicates that a layer of reduced density is not specific to water, but it depends—as discussed below—on the relative affinity between the substrate and the liquid.

The relative affinity of a surface and a liquid is correlated with the interfacial energy, $\gamma_{sl} = \gamma_{sg} - \gamma_{lg} \cos \vartheta$, where γ_{sg} is the surface energy of the solid surface, γ_{lg} the surface tension of the liquid, and ϑ is the contact angle between the liquid and the solid surface. The surface energies of the thiol-modified surfaces used in our work (C_{12}, $C_{12}/C_{11}OH$, C_{16}) were taken from ref 15, and the contact angles were measured in our laboratory (Table 5). The D and ΔD measured in our experiments at the more hydrophobic surfaces (C_{12} and C_{16}) are between 1 and 2 Å, and the interfacial energies between the solids and the aqueous phase is about 47 mJ/m^2. This is in fair agreement with the results obtained for polystyrene film in contact with D_2O,[9] for which the interfacial energy is about 44 mJ/m^2 and the depletion distance D is ∼2.4 Å, and those obtained for a paraffin film in contact with water[13] where the interfacial energy is ∼50 mJ/m^2 and the D is 1 Å. The contact angles and the surface energy of polystyrene and paraffin, the samples used in refs 9 and 13, were taken from the literature[44,45] (Table 5). It must be noted, however, that a direct comparison between the results obtained with different experiment/sample systems is not straightforward since the different experiments had also different sensitivities, e.g., the low X-ray scattering contrast between the aqueous and the organic phase.[11,46]

Table 5. Surface Energy and Contact Angle of the Surfaces Used in Our Experiments and in the Experiments of Refs 9 and 13[a]

sample	γ_{sg} (mJ/m^2)	ϑ	liquid	γ_{lg} (mJ/m^2)	γ_{sl} (mJ/m^2)
C_{12}	23.2[15]	109°	water	72.75	46.8
C_{12}	23.2	35°	cyclohexane	25.5	2.3
C_{12}	23.2	30°	*n*-octane	21.8	4.3
$C_{12}/C_{12}OH$	58[15]	45°	water	72.75	6.5
$C_{12}/C_{12}OH$	58	<10°	toluene	28.5	29.7
C_{16}	17.6[15]	110°	water	72.75	47.1
polystyrene[9]	43	91°	water	72.75	44.2
paraffin[13]	25	111°	water	72.75	48−52

[a] The surface energy of the C_{12}, $C_{12}/C_{12}OH$, and C_{16} were taken from ref 18; the contact angle and surface energy of polystyrene and paraffin were taken from refs 44 and 45, respectively. The interfacial energy was calculated by considering that $\gamma_{sl} = \gamma_{sg} - \gamma_{lg} \cos \vartheta$, where γ_{sg} is the surface energy of the solid surface, γ_{lg} the surface tension of the liquid, and ϑ the contact angle between the liquid and the solid surface.

The difference in the interfacial energies upon exposure of the hydrophobic samples S1 and S2 to water and nonpolar solvents, $\Delta\gamma_{C12} = \gamma_{C12,water} - \gamma_{C12,nonpol}$, are 44.5 and 42.5 mJ/$m^2$ for cyclohexane and *n*-octane, respectively, which correspond to a difference in ΔD of 1.3 and 1.5 Å. In the case of the more hydrophilic sample S3, the difference in the interfacial energy $\Delta\gamma_{C12/C11OH} = \gamma_{C12/C11OH,water} - \gamma_{C12/C11OH,nonpol}$ is −23.3 mJ/m^2 corresponding to a ΔD of −1.8 Å. Therefore, the density deficit of a liquid at a solid surface appears to be correlated with the relative affinity of the liquid and the solid phase. This result is in qualitative agreement with the computer simulations, which predict $\Delta D = 0.34$ Å for a nonpolar substrate in contact with water and cyclohexane, and $\Delta D = -0.79$ Å for a polar substrate in contact with water and toluene. In the case of the fully deuterated hexadecanethiolate SAM (S4), the depletion distance, D, obtained for water in the simulation and in the experiment against D_2O at 25 °C, is 1.64 and 1.6−2.2 Å, respectively.

Influence of pH, Electrolytes, and Temperature on the Depletion Layer. The effect of pH and electrolytes was studied to determine whether the depletion layer is affected by these parameters. Since the errors in D are larger than the variation caused by the change in pH or by the presence of electrolytes, caution must be taken when interpreting the results. Measurements at pH 5 and 2 show that the effect of the surface charge on the extension of the depletion layer is minor. This result indicates that the formation of a density depleted liquid layer at the SAM−water interface is not strongly correlated to the reorientation of the water dipoles next to the SAM upon change of pH.

(41) See, Y.-S.; Satija, S. *Langmuir* **2006**, *22*, 7113−7116.
(42) Zolk, M.; Eisert, F.; Pipper, J.; Herrwerth, S.; Eck, W.; Buck, M.; Grunze, M. *Langmuir* **2000**, *16*, 5849−52.
(43) Hui Hong, T.; Davies P. B. *Langmuir* **1993**, *9*, 1836−45.
(44) Owens, D. K. *J. Appl. Polym. Sci.* **1969**, *13*, 1741−47.
(45) Israelachvili, J. N. *Intrermolecular and surface forces*; Academic Press: San Diego, 1989.

The addition of salts causes a slight increase in the depletion distance, D, both for potassium sulfate and for calcium chloride. Interestingly, the effect of the added salts points in the same direction although potassium sulfate is a "structure former" and calcium chloride is a "structure breaker". This implies that the reduced water density found at the hydrophobic surfaces is not correlated to the Hofmeister series of salts. A trend is, however, observed with the surface tension of the liquid, which increases if salts are added. If γ_w^0 is the surface tension of pure water at room temperature, the relative increase in surface tension is $\gamma/\gamma_w^0 = 1.006$ and 1.011 for 0.25 M solutions of K_2SO_4 and $CaCl_2$, respectively.[47,48] Thus, the increase of the water surface tension (and hence interfacial tension) correlates within the error bars to an enlarged depletion layer.

The experiments conducted as a function of temperature show that the extension of the depletion layer increases with temperature. The experiments were performed with a thicker SAM in order to reduce the ratio between the roughness and the thickness of the organic monolayer, and although the Nevot−Croce approach could still not be used, the SAM layer could be explicitly considered in the model. However, also in this case, the SAM was at the limit of resolution of the NR experiment. To overcome this problem, it was necessary to apply more global fitting strategies by fixing the thickness of the SAM to the measured ellipsometric value (achieved by spectral ellipsometry) and by fitting its SLD (fitting method I). Alternatively, both the thickness and the SLD of the SAM were fitted, constrained by the condition that the sum of the thickness of the Au layer plus SAM was equal to the value measured in the vacuum NR measurement (fitting method II). Although the absolute extension of the depletion layer is sensitive to the fit procedure used, its trend with temperature is the same and consistent with the MC simulation.

With rising temperature, the surface tension of water decreases,[49] and we would actually expect a decrease in depletion distance as discussed above in the context of the addition of salts. The temperature dependence observed in our experiment, however, is in agreement with the theoretical work of Lum and Chandler[4] who showed that the extension of the depletion layer should increase when the boiling point is approached. Obviously, to explain the extension of the depletion layer as a function of temperature, two opposing effects have to be taken into account. One is the interfacial energy difference which will decrease with temperature and reduce the depletion layer, the other is the energy required to transfer a water molecule from the liquid to the vapor phase. This can be estimated by considering the chemical potential (molar Gibbs free energy) difference between liquid water and its vapor phase, $\mu_g - \mu_l$, which decreases with temperature. As the temperature raises, the energy associated to the transition liquid−vapor of a water molecule decreases, and consequently the depletion layer increases.

In Table 6 we list the values $\mu_g - \mu_l/\mu_g^\circ - \mu_l^\circ$ and γ/γ° (25 °C) in order to evaluate the relative variation of the two terms as a function of the temperature and in the presence of electrolyte. μ_g, μ_l, μ_g°, μ_l° refer to the chemical potential of vapor and water and their standard values, respectively. Aqueous solutions of the electrolytes have a higher surface tension and a higher difference $\mu_g - \mu_l$ in comparison with pure water. With increasing temperature both γ_w and $\mu_g - \mu_l$ decrease, which has an opposing effect on the extension of the depletion layer. The dominant effect seems to be the change in chemical potential difference, since, as the temperature increases from 6 to 50 °C, $\mu_g - \mu_l$ decreases by 50% and γ by 8%, respectively. The fact that two terms contribute in opposite fashion to the extension of the depletion layer might also explain the small variation measured experimentally.

Table 6. The Variations, $\mu_g - \mu_l$, and the Surface Tension of Water, γ, Normalized to Their Respective Values at 25 °C[a]

	$(\mu_g - \mu_l)/(\mu_g^\circ - \mu_l^\circ)$	γ/γ_w^0 (25 °C)
$CaCl_2$ (0.25 M)	1.0035	1.011
K_2SO_4 (0.25 M)	1.003	1.006
$T = 6$ °C	1.2	1.02
$T = 25$ °C	1	1
$T = 50$ °C	0.6	0.94

[a] The surface tension of water as a function of the temperature[52] and in the presence of potassium sulfide and calcium chloride were taken from the literature.[47,48] The contribution of the bulk free energy was estimated by taking from literature the chemical potential (molar Gibbs energy) of vapor and of water as a function of temperature[53] and the chemical potential of water in the presence of dissolved salts, which could be estimated from water activity.[54]

Comparison with Force Measurements. The presence of a region of water with reduced density at extended nonpolar surfaces is thought to be the origin of the hydrophobic force between hydrophobic bodies.[4] We can attempt to correlate the extension of the depletion layer with the range of forces measured between hydrophobic surfaces. Several surface force measurements can be found in the literature, and many of them show contradictory results which are difficult to rationalize.[50] Experiments performed with different surfaces exhibit significantly different ranges and magnitudes of the attractive force. It is therefore important to compare experiments performed on identical or at least similar surfaces. Surface force measurements performed with an atomic force microscope on hexadecanethiol-modified gold surfaces[51] show no interaction as long as the surfaces are at a distance larger than several nanometers until they jump into contact. The jump-in distance is around 5 nm in pure water at room temperature. This is fairly close to two times the extension of the depletion layer, d_L, of water on hexadecanethiol monolayers (sample S4) at $T = 25$ °C (see Table 3). The strong attraction seems to occur when the interfacial low-density regions of water adjacent to each surface overlap. Measurements performed with the addition of several salts show an increase of the jump-in distance,[51] also in agreement with our results that show an increased depletion zone in the presence of salts.

We emphasize that the extension of the interfacial water layer is at the resolution limit of the NR experiments, and measuring its thickness and density is a formidable task. This limitation is reflected in the large error bars that affect the depletion distances, D. However, the simulations performed for this system as a function of temperature give the same trend as the experimental data and thus support the overall experimental observations.

Conclusions

From the NR experiments conducted on SAMs in polar and nonpolar liquids, further evidence is found for the existence of liquid density depleted boundary layers. Such interphases are formed at hydrophobic SAMs (water contact angle 107°) against

(46) Ball, P. *Nature (London)* **2003**, *423*, 25.
(47) Abramzon, A. A.; Gankhberg, R. D. *Zh. Prikl. Khim.* **1993**, *66*, 1665−74.
(48) Abramzon, A. A.; Gankhberg, R. D. *Zh. Prikl. Khim.* **1993**, *66*, 1428−38.
(49) Jhon, Mu Shik; Van Artsdalen, E. R.; Grosh, J.; Eyring, H. *J. Chem. Phys.* **1967**, *47*, 2231−4.
(50) Christenson, H. K.; Claesson, P. M. *Adv. Colloid Interface Sci.* **2001**, *91*, 391−436.
(51) Kokkoli, E.; Zukoski, C. F. *Langmuir* **1998**, *14*, 1189−95.
(52) Keiser, W. V. *J. Colloid Interface Sci.* **1976**, *56*(3), 622.
(53) Job, G.; Herrmann, F. *Eur. J. Phys.* **2006**, *27*, 353−371.
(54) El Guendouzi, M.; Dinane, A.;and Mounir, A. *J. Chem. Thermodyn.* **2001**, *33*, 1059−1072. El Guendouzi, M.; Mounir, A.; Dinane, *J. Chem. Thermodyn.* **2003**, *35*, 209−220.

water but also at hydrophilic SAMs (water contact angle 45°) against nonpolar fluids. The findings suggest that the density deficit of a fluid is not unique to aqueous solid−liquid interfaces but is more general and correlated with the affinity of the liquid phase to the solid phase. Experiments conducted at the same solid−liquid interface at different pH showed minor influence on this parameter, and we conclude that effects as the reorientation of water dipoles do not contribute significantly on the extension of the depletion layer. Measurements performed in the presence of electrolytes and as a function of temperature show that the extension of the depletion layer is governed by at least two parameters: (i) the surface energy difference of the solid and liquid that determines the energetic cost of having a water molecule in contact with the surface and (ii) the temperature- and solute-dependent free energy of the liquid water phase in relation to that of the vapor, which determines the energy cost of transferring a water molecule from the liquid to the vapor phase.

The smaller both differences are, the more compatible is water with the substrate and the steeper is the density gradient of the liquid in the interphase.

The results of the experiment are in good agreement with Monte Carlo simulations performed on similar systems. Although no profound statement on absolute extension and absolute depletion can be made since the analysis is close to the limit of what can be done with NR, the extracted relative parameter D and ΔD are within the range of other published data on comparable systems and give further evidence of the existence of water density depletion at hydrophobic surfaces.

Acknowledgment. The authors thank G. Albert for preparing the Au films on the substrates and G. Meinusch, R. Jehle, and W. Weis for technical assistance. BENSC at HMI and the ILL are gratefully acknowledged for access to facilities and financial support. We acknowledge the financial support of Helmholtz Association of National Research Centres (HGF), within the framework of the Virtuelle Institut "Funktionelle Eigenschaften Aquatischer Grenzflächen" Bonn, Germany, the EU Strep Nanocues, and the Office of Naval Research.

Supporting Information Available: Fitting and force field parameters. This material is available free of charge via the Internet at http://pubs.acs.org.

LA061943Y